

# Vertical habitat utilization by large pelagic animals: a quantitative framework and numerical method for use with pop-up satellite tag data

JIANGANG LUO,<sup>1</sup> ERIC D. PRINCE,<sup>2</sup>  
C. PHILLIP GOODYEAR,<sup>3</sup> BRIAN E.  
LUCKHURST<sup>4</sup> AND JOSEPH E. SERAFY<sup>2\*</sup>

<sup>1</sup>Division of Marine Biology and Fisheries, Rosenstiel School of Marine and Atmospheric Science, University of Miami, Miami, FL, USA

<sup>2</sup>Southeast Fisheries Science Center, National Marine Fisheries Service, Miami, FL, USA

<sup>3</sup>1214 N. Lakeshore Drive, Niceville, FL, USA

<sup>4</sup>Marine Resources Division, Department of Environmental Protection, Crawl CRBX, Bermuda

## ABSTRACT

A quantitative framework and numerical methodology were developed to characterize vertical habitat utilization by large pelagic animals and to estimate the probability of their capture by certain types of fishing gear. Described are the steps involved to build 'vertical habitat envelopes' from data recovered from an electronically tagged blue marlin (*Makaira nigricans*) as well as from a longline fishing gear experiment employing temperature–depth recording devices. The resulting vertical habitat envelopes, which integrate depth and temperature preferences of tagged fish, are conducive for comparative studies of animal behavior and for calculation (and visualization) of degrees of overlap – be it among individuals, species or fishing gear. Results of a computer simulation evaluation indicated our numerical procedure to be reliable for estimating vertical habitat use from data summaries. The approach appears to have utility for examining pelagic longline fishing impacts on both target and non-target species and could point to ways of reducing bycatch via modification of fishing strategy or gear configuration.

**Key words:** blue marlin, numerical estimation, satellite tags, vertical habitat.

\*Correspondence. e-mail: joe.serafy@noaa.gov

Received 24 June 2004

Revised version accepted 7 April 2005

## INTRODUCTION

While critical for defining, assessing and ultimately managing fish stocks, relevant data on fish movement (e.g. migration pathways, foraging behavior, habitat preferences) are among the most difficult and expensive to obtain. Quantifying the movements of large pelagic fishes, such as the billfishes (Istiophoridae), is particularly challenging given their low densities, highly migratory behavior and the vast, dynamic nature of the environment that they inhabit. Until recently, most of what is known about billfish movement has been gleaned from conventional (e.g. plastic streamer) tags that have been attached and recovered by fishers (Ortiz *et al.*, 2003). If recovered, these tags can reveal little more than the net distance traveled and time elapsed between tagging and recovery location – the path taken, including the depths visited by the fish, are unknown. New electronic tagging technologies, however, are helping to reveal aspects of pelagic fish behavior as never before (see Sibert and Nielsen, 2001 and papers therein; Jonson *et al.*, 2003). Among the most significant developments is the pop-up satellite archival transmitting (PAT) tag (Block *et al.*, 2001). Once attached to a fish, current PAT tag technology can: (i) sample temperature, depth (pressure) and light levels at user-defined time intervals (e.g. seconds to minutes) and then store and process these data; (ii) detach from its bearer after a user-defined time duration (e.g. weeks to months); and (iii) after floating to the surface, transmit either raw data or processed summaries of their archived information to satellites, which subsequently communicate these data back to the research team. As PAT tags eliminate the need for recovery of the tag itself, they represent a truly fishery-independent means of obtaining movement data on pelagic fishes in their natural environment.

Increasingly, PAT tags are being used to gather data on horizontal and vertical movements of pelagic fishes in relation to conditions and/or features of their biophysical environment (Brill and Lutcavage, 2001; Brill *et al.*, 2002) as well as to address questions of post-release mortality (Graves *et al.*, 2002; Kerstetter *et al.*,

2003). In practice, however, there is great uncertainty when estimating the horizontal movement track of a PAT-tagged fish, because longitude and latitude must be inferred from underwater light levels, and these are subject to great variation at any given location (Musyl *et al.*, 2001). In contrast, characterizing the vertical movement of PAT-tagged fishes in sea water is relatively clear-cut. This is because, given concurrent temperature and pressure measurements made by the tag (and assuming near-constant oceanic salinity conditions), depth can be estimated with a high degree of accuracy and precision (manufacturers claim sensor depth and temperature resolution are 0.5 m and 0.05°C, respectively). Species-specific knowledge of vertical habitat utilization is especially important when considering high-seas fishing impacts on populations of targeted fishes as well as those caught as bycatch. To date, however, relatively little has been done with PAT tag-collected data to characterize depth and temperature preferences of pelagic fishes beyond simple plots of depth and temperature versus time and/or histograms of total time spent within depth and temperature bins.

We present a quantitative approach towards vertical habitat characterization that integrates the thermal and depth preferences of one or more PAT-tagged animals. The method enables the construction of three-dimensional 'vertical habitat envelopes' from summarized or raw PAT tag data streams, which in principle are conducive for making temporal, spatial, gender, size and/or species comparisons as well as for quantifying the probability of encounter with certain types of fishing gear. In this paper, we first provide a detailed description of data and the algorithm. Second, we evaluate the algorithm with simulated depth and temperature data. Third, we calibrate the algorithm with minute-by-minute depth and temperature data from a physically recovered PAT tag that was attached to an Atlantic blue marlin (*Makaira nigricans*) for 38 days and that also successfully communicated its data, in summary form, back to our research team. Finally, we provide an example of the potential utility of this approach for quantifying animal-gear interactions.

## METHODS

There are currently two PAT tags available on the market: one manufactured by Microwave Telemetry (MT, Columbia, MD, USA) and the other by Wildlife Computers (WC, Redmond, WA, USA). Both communicate with the ARGOS satellite system and have similar external appearances, sensors, sampling

frequency capabilities, power requirements and transmission rates. Where the MT and WC tags differ is in how they handle their respective data streams, which ultimately affects the resolution of data and the duration for which each tag type can be usefully deployed. In this study, we describe data and methods as they apply to WC-PAT tags. The approach designed into this tag type is to perform data summarization 'onboard' the tag to reduce the size of the data set which needs to be transmitted. This allows for deployment durations of months rather than days. Although only summarized data are transmitted, the archived data set is still retained in its entirety in the rare event that the tag is physically recovered.

### Data and algorithm description

For each user-defined time block (e.g. 1, 3, 6, or 12 h), the WC tag data processing software (i) computes the proportion of time the tag spent within 12 user-defined depth bins ( $D$ ), (ii) computes the proportion of time the tag spent within 12 user-defined temperature bins ( $T$ ), and (iii) extracts temperature and depth minima and maxima at eight depth intervals that range between, and are inclusive of, the shallowest and the deepest depth visited by the fish (i.e. depth-temperature profile, DTP). The tag software also extracts portions of the light-level data that encompass sunset and sunrise for purposes of horizontal geolocation estimation; however, these data are not considered in this paper. Characterization of the vertical habitat of WC-PAT-tagged animals is usually depicted in separate time-at-temperature and time-at-depth histograms (Fig. 1a,b respectively) and/or plots with depth and temperature minima and maxima on the  $y$ -axis and time on the  $x$ -axis. In some cases, depth-temperature profiles (Fig. 1c) showing vertical temperature distributions as sampled by the PAT tag are also presented. While it is critical to consider each separately, we saw utility in also integrating the  $D$ ,  $T$  and DTP summary information into a depth-temperature matrix of time (DTM) or 'vertical habitat envelope' matrix (Table 2). Specifically, each matrix has a  $12 \times 12$  structure (corresponding to the 12 temperature and 12 depth bins defined by the user), and each cell represents the proportion of time (e.g. average time, total time) spent by the tagged animal at each temperature-depth combination. If a tag is physically recovered, it is possible to create the DTM by simply summing and tabulating the amount of time for each cell from the minute-by-minute data records for each pooled time interval (e.g. 6 h). However, physical recovery of a given PAT tag is exceedingly rare, and

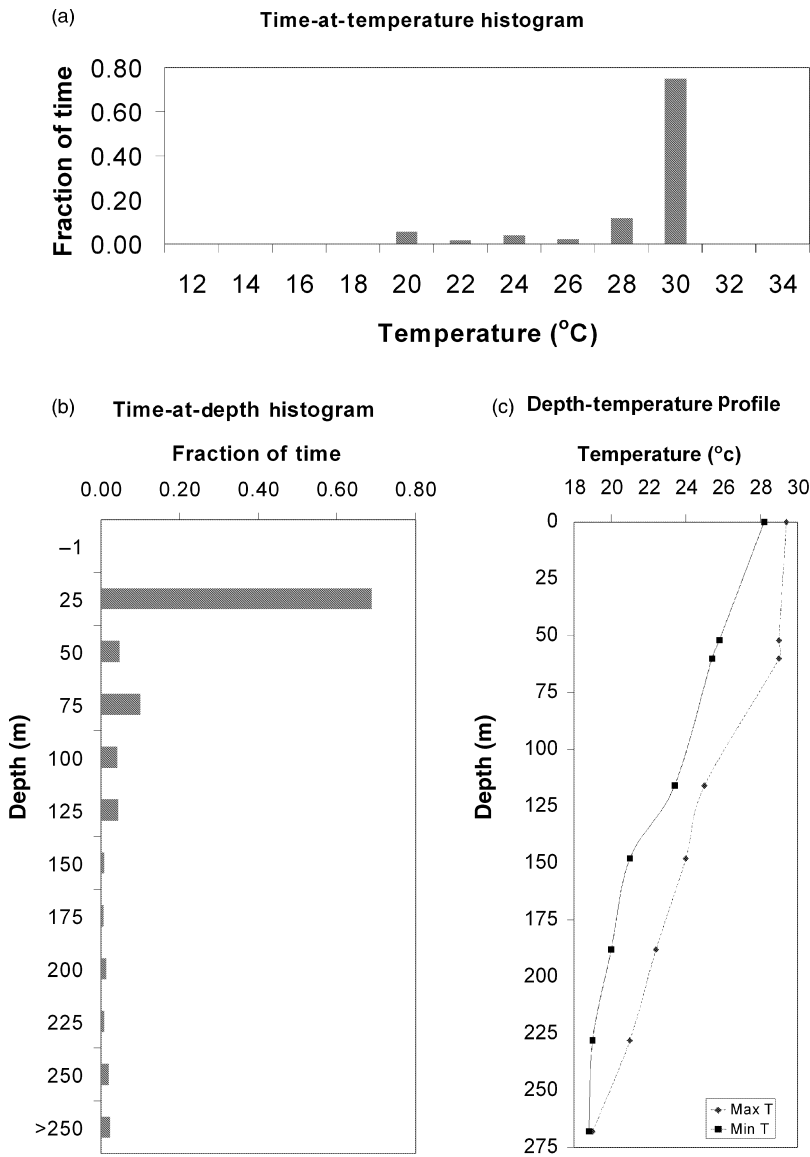


**Figure 1.** Examples of satellite-transmitted data summaries: (a) time-at-temperature histogram,  $T$ ; (b) time-at-depth histogram,  $D$ ; and (c) depth-temperature profile DTP.

there is no algebraic solution for calculating the DTM from the summarized data alone. To address these problems, we used a Bayesian approach to develop a numerical approximation scheme for estimating the DTM from summarized data. The scheme incorporates the following algorithms.

The time-at-depth histogram for a time interval can be expressed as a prior probability density function  $P[D]$ :

$$P[D] = [d_0, d_1, d_2, \dots, d_j, \dots, d_{11}], \quad (1)$$

where  $d_j$  is the fraction of time the fish spent at depth bin  $j$ , and  $\sum_{j=0}^{11} d_j = 1$ . The depth bin ranges (in meters) for this study were programmed prior to the PAT tag deployment as:

$$D_{\text{bin}(j)} = [-40 - -1, 0 - 25, 26 - 50, 51 - 75, 76 - 100, 101 - 125, 126 - 150, 151 - 175, 176 - 200, 201 - 225, 226 - 250, 251 - 1000].$$

The first depth bin was set to the negative value because the software on the PAT tag uses this to correct the depth sensor drift.

The time-at-temperature histogram for a time interval can be expressed as a prior probability density function  $P[T]$ :

$$P[T] = [t_0, t_1, t_2, \dots, t_i, \dots, t_{11}], \quad (2)$$

where  $t_i$  is the fraction of time the fish spent at temperature bin  $i$ , and  $\sum_{i=0}^{11} t_i = 1$ . The temperature bin

ranges (°C) for this study were programmed prior to the PAT tag deployment as:

$$T_{\text{bin}(i)} = [-1 - 12, 12.1 - 14, 14.1 - 16, 16.1 - 18, \\ 18.1 - 20, 20.1 - 22, 22.1 - 24, 24.1 - 26, \\ 26.1 - 28, 28.1 - 30, 30.1 - 32, 32.1 - 60].$$

The DTP data can be expressed as three arrays:

$$PD = [pd_0, pd_1, \dots, pd_k, \dots, pd_7], \quad (3)$$

$$PT_{\text{min}} = [tm_0, tm_1, \dots, tm_k, \dots, tm_7], \quad (4)$$

$$PT_{\text{max}} = [tx_0, tx_1, \dots, tx_k, \dots, tx_7], \quad (5)$$

where  $pd_k$  is the depth in meters,  $tm_k$  is the minimum temperature and  $tx_k$  is the maximum temperature (°C) of DTP bin  $k$ . We linearly interpolated the minimum and maximum temperatures from the DTP data to create a 2-by-12 array of minimum and maximum temperatures that matched the 12 depth bins of the time-at-depth histogram:

$$\text{DTP} = \begin{bmatrix} T_{\text{min}(0)} & T_{\text{max}(0)} \\ \vdots & \vdots \\ T_{\text{min}(j)} & T_{\text{max}(j)} \\ \vdots & \vdots \\ T_{\text{min}(11)} & T_{\text{max}(11)} \end{bmatrix}. \quad (6)$$

The DTM is defined as a two-dimensional array of  $12 \times 12$  elements:

$$\text{DTM}(i, j) = \begin{bmatrix} a_{0,0} & \cdots & a_{i,0} & \cdots & a_{11,0} \\ \vdots & & \vdots & & \vdots \\ a_{0,j} & \cdots & a_{i,j} & \cdots & a_{11,j} \\ \vdots & & \vdots & & \vdots \\ a_{0,11} & \cdots & a_{i,11} & \cdots & a_{11,11} \end{bmatrix}, \quad (7)$$

where  $a_{i,j}$  is the fraction of time that the fish spent in temperature bin  $T_{\text{bin}(i)}$  and depth bin  $D_{\text{bin}(j)}$  for the time interval, and can be expressed as a joint probability of  $P[T_i \text{ and } D_j]$ :

$$a_{i,j} = P[T_i \text{ and } D_j] = P[T_i] \cdot P[D_j|T_i] = P[D_j] \cdot P[T_i|D_j]. \quad (8)$$

From Bayes' Theorem (Baskin, 1986) we have:

$$P[D_j|T_i] = P[D_j] \cdot P[T_i|D_j] / \sum_j P[D_j] \cdot P[T_i|D_j], \quad (9)$$

$$P[T_i|D_j] = P[T_i] \cdot P[D_j|T_i] / \sum_i P[T_i] \cdot P[D_j|T_i], \quad (10)$$

where  $P[T_i]$  and  $P[D_j]$  are observed and  $P[D_j|T_i]$  and  $P[T_i|D_j]$  are unknown. Substitute eqn 8 into eqns 9 and 10, and we have:

$$P[D_j|T_i] = a_{ij} \sum_j a_{ij} \quad (11)$$

$$P[T_i|D_j] = a_{ij} \sum_i a_{ij}. \quad (12)$$

Based on the above Bayes' formula, we developed a computer algorithm to iteratively estimate the DTM with IDL software (Interactive Data Language; Research Systems Inc., Boulder, CO, USA). We first initialize the temperature distribution of each depth bin (i.e.  $P[T_i|D_j]_{k=0}$ ) with a type of probability distribution  $H$  between the minimum and maximum temperature of the depth bin provided by the DTP. Three types of  $H$  (uniform, normal, and triangle) were examined (Fig. 2a). Certain parameters are required to generate random values for the three initial functions. For the uniform function, only minimum ( $a$ ) and maximum ( $b$ ) temperatures are required whereas median temperature ( $c$ ) is also required for the triangle function. For the normal function, the mean ( $u$ ) and standard deviation ( $\sigma$ ) are required, which were approximated by  $u = (a + b)/2$  and  $\sigma = (b - a)/4$ . The uniform and triangle functions generate values between  $a$  and  $b$ , while the normal function generates values between  $\pm\infty$ . Thus, the tails of the normal function were truncated at  $a$  and  $b$ . For simplicity, we used the uniform distribution as an example here. We first used the random uniform function (RANDOMU) from the IDL function library to generate 360 (minutes in 6 h) random temperatures ( $T_{\text{ran}}$ ) between the minimum ( $T_{\text{min}}$ ) and maximum ( $T_{\text{max}}$ ) temperatures from DTP:

$$T_{\text{ran}} = T_{\text{min}} + (T_{\text{max}} - T_{\text{min}}) * \text{RANDOMU}(\text{seed}, 360),$$

where 'seed' is an integer variable for the random number generator. Next, we used the HISTOGRAM function to make a probability density function which matches the bin size of the  $P[T]$ :

$$H = \text{HISTOGRAM}$$

$$(T_{\text{ran}}, \text{min} = 10, \text{max} = 32, \text{bin} = 2)/360,$$

where  $P[T_i|D_j]_{k=0} = H$ . Then, with eqn 8, we initialized the DTM as:

$$\hat{a}_{ij,k=0} = P[D_j] \cdot H. \quad (13)$$

We substituted  $a_{ij}$  in eqn 11 with  $\hat{a}_{ij,k=0}$  to estimate  $P[D_j|T_i]_{k=1}$ :

$$P[D_j|T_i]_{k=1} = \hat{a}_{ij,k=0} / \sum_j \hat{a}_{ij,k=0} \quad (14)$$

and substituted  $P[D_j|T_i]_{k=1}$  into eqn 8 to estimate  $\hat{a}_{ij,k=1}$ :

$$\hat{a}_{ij,k=1} = P[T_i] \cdot P[D_j|T_i]_{k=1} \quad (15)$$

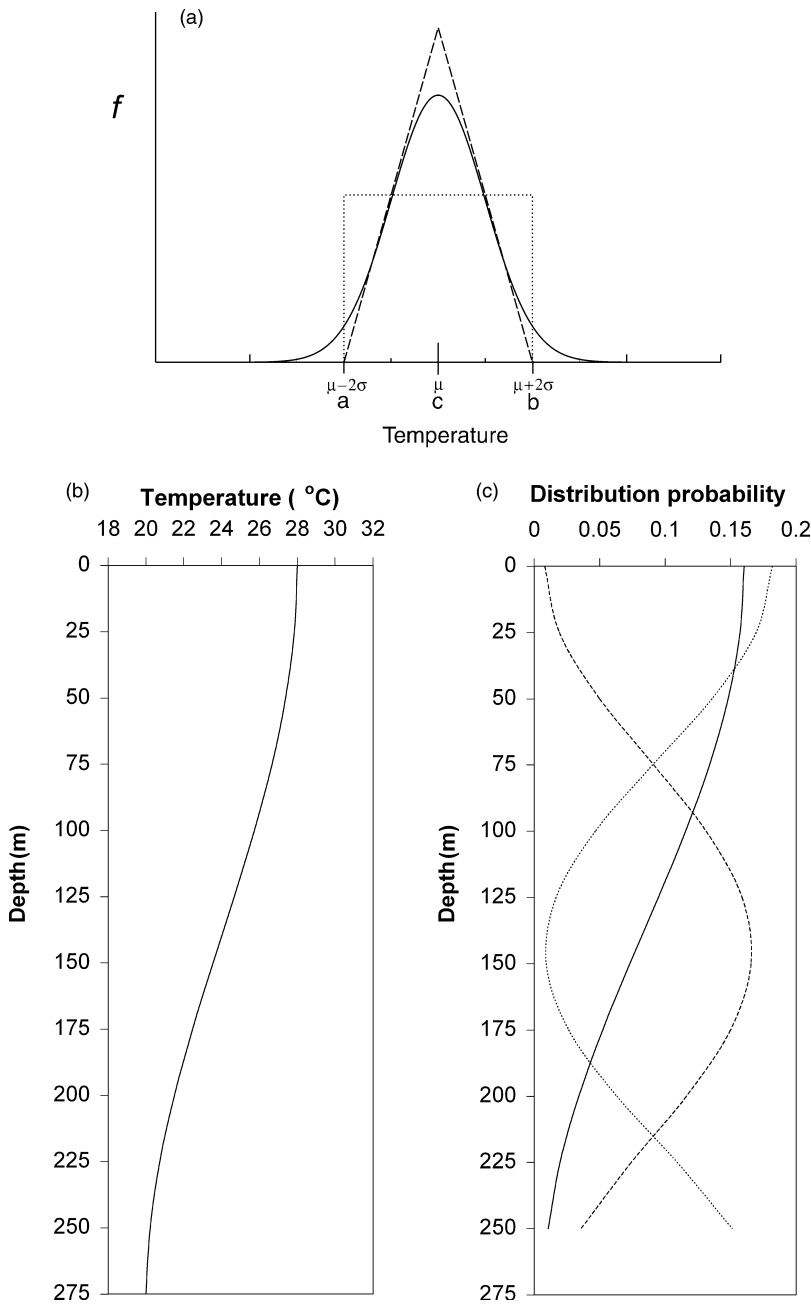


**Figure 2.** (a) Three types of initial temperature distribution functions (normal solid, triangle dashed, uniform dotted), (b) hypothetical vertical temperature distribution, (c) three hypothetical vertical probability density distributions for the fish (i.e. DP1 solid, DP2 dotted, DP3 dashed).

and substituted  $\hat{a}_{ij,k=1}$  into eqn 12 to estimate  $P[T_i|D_j]_{k=1}$ :

$$P[T_i|D_j]_{k=1} = \hat{a}_{ij,k=1} / \sum_i \hat{a}_{ij,k=1} \quad (16)$$

and substituted  $P[T_i|D_j]_{k=1}$  into eqn 8 to make another estimate of  $\hat{a}_{ij,k=1}$ :

$$\hat{a}_{ij,k=1} = P[D_j] \cdot P[T_i|D_j]_{k=1}. \quad (17)$$

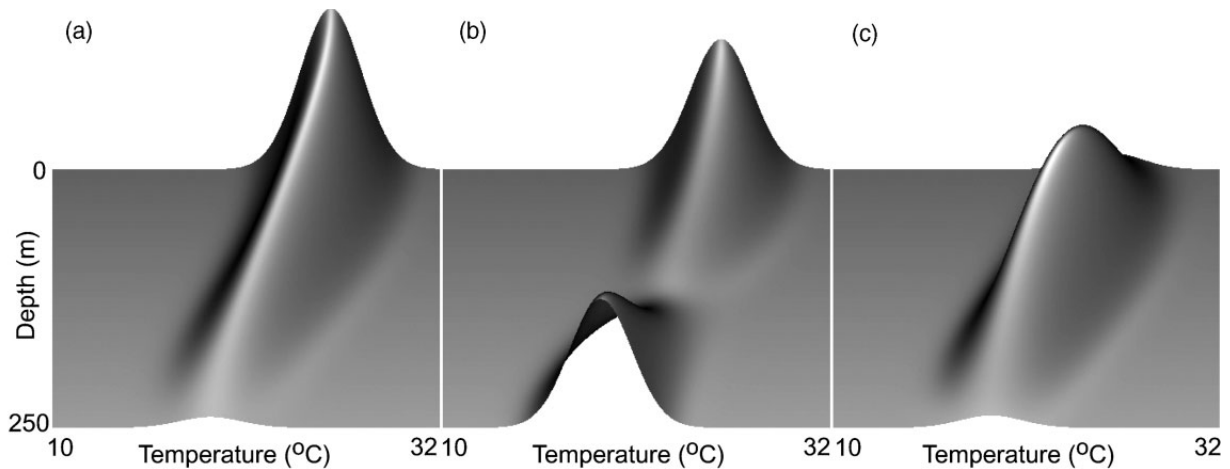
We then applied eqns 14 through 17 sequentially until  $P[T]$  and  $P[D]$  are arbitrarily close to  $\sum_j \hat{a}_{ij}$  and

$\sum_i \hat{a}_{ij}$  or the simulation step  $k$  equal to 1000. The complete routine written in IDL is provided in Appendix 1.

*Algorithm evaluation*

We first used a simple example to validate the performance of the algorithm (Appendix 2). Then, we used computer simulation to test the algorithm for a variety of plausible time-at-depth, time-at-temperature, and DTP configurations. At two extreme

**Figure 3.** Joint bivariate probability density function for three hypothetical vertical fish distributions at  $\sigma = 2.0$ : (a) DP1; (b) DP2, and (c) DP3.



situations, specifically when (i) temperature is uniform within the water column, or (ii) a pelagic animal remains at a constant depth, we can determine the DTM without estimation. For the purpose of illustration, we assumed a vertical mean temperature profile (Fig. 2b) with a normal temperature probability density function for each depth bin, and three depth-distribution probability density functions  $P[D]$  (Fig. 2c, DP1, DP2 and DP3). Combining the temperature and depth-distribution probability functions, we have a bivariate joint probability density function  $pdf(T, D)$  for each depth function (Fig. 3). We randomly simulated the temperature distribution for each depth bin at four levels of temperature variation ( $\sigma = 0.25, 0.5, 1.0, 2.0$ ) to make a hypothetical 'true' DTM for each of the 12 scenarios (3 depth profiles  $\times$  4 temperature variation scenarios). From the 'true' DTM, we calculate  $P[T]$  and DTP with 0.5% truncation of each tail. Then, we used  $P[D]$ ,  $P[T]$ , and DTP as inputs to our algorithm to make an estimated matrix (DTMX) of the corresponding 'true' DTM with three different initial temperature distribution functions (Fig. 2a).

#### Algorithm calibration

We also calibrated the algorithm using data collected while the tag was attached to a real fish. The computer algorithm to estimate DTM is useful because typically only  $D$ ,  $T$ , and DTP data are available to researchers using WC-PAT tags. However, on June 3, 2003, our research team was very fortunate to physically recover a WC-PAT tag that (i) was attached to a blue marlin in the vicinity of St Thomas, US Virgin Islands on Oct 12, 2002; (ii) recorded and archived depth, tem-

perature and light levels for over 56 000 consecutive minutes; and (iii) detached about 800 km SSW of the tagging location off the coast of Honduras where it successfully communicated its summary data (i.e.  $D$ ,  $T$  and DTP) via the satellite system. Excluding the data from the first and last incomplete days, we have 38 complete days of data. We divided the minute-by-minute data into 6-h intervals to match the summary data transmitted via satellite. Next, we calculated the true DTM with the minute-by-minute data for each 6-h time window. Then, we estimated each DTMX from summarized data with the mean of 100 runs of the algorithm routine for the same 6-h window. As a result, we have 152 (38 days  $\times$  4 time windows) pairs of comparison between the estimated DTMX and the true DTM.

#### Application

Finally, we combined the above matrices of diel vertical habitat utilization with similar matrices that depict the vertical distribution and intensity (i.e. soak time) of fishing to show the potential utility of this approach for quantifying animal-gear interaction probabilities. The gear depth-temperature envelopes were generated from data collected by miniature temperature-depth recording instruments that were deployed on independent longline gear experiments (P. Rice, University of Miami, Florida, unpublished data). We conducted an experimental longlining cruise during which miniature temperature-depth recording instruments (TDRs) were deployed near the hooks of a longline. In the experiments, the mainline was 46-km long with 10-m floatlines, 12-m gangions and 560 baited hooks. A TDR was placed about 1.8 m

above (i.e. proximal to) every 13th hook. Use of the TDRs allowed us to construct a DTM for this gear. Subsequently, we calculated, purely for illustrative purposes, the theoretical time that fish and hooks would have overlapped had the two DTMs been coincident by element-to-element multiplication of the gear DTM with each 6-h window of fish habitat DTM.

## RESULTS

In the simulation experiment, we ran 1000 simulations for each combination of  $P[D]$  and sigma with three initial temperature distribution functions described in the Methods section. To compare the difference in minutes per 6 h between DTMX and DTM, we first calculated the absolute difference matrix  $[ADM(i, j) = |DTMX(i, j) - DTM(i, j)|]$  for each simulation, then calculated the sum  $[Sm = \sum_{ij} ADM(i, j)]$  and maximum ( $Mx = \text{Max}\{ADM\}$ ) for each ADM. For each scenario, we calculated the mean and standard deviation of Sm and Mx ( $N = 1000$ ). The sum of the absolute difference (Sm) is an indication of estimation bias for the overall performance of the algorithm (Table 1a), while Mx indicates the estimation bias for an individual cell (Table 1b). As the temperature variation ( $\sigma$ ) of the 'true' DTM increased, Sm increased under all scenarios, while Mx did not

increase when  $\sigma > 1$ . This is because the number of non-zero cells in the matrix increases as  $\sigma$  increases, which enlarges the number of cells that need to be estimated in the simulation, and spreads the total time over more cells. Therefore, the cumulative bias over all the cells (Sm) increases.

Comparing among the three depth-distribution profiles of the 'true' DTM (Table 1a), the differences in Sm values are small when estimation was carried out with the normal and the triangle initial temperature distribution functions and are much larger with the uniform function, especially when  $\sigma > 0.25$ . Specifically, the DP3 profile is the least biased and DP2 profile is the most. This difference emerges as the vertical temperature profile (Fig. 2b) and the vertical fish distribution profiles are combined (Fig. 2c). The algorithm can solve 24 exact cell values (with no bias) when they are arranged perfectly as two cells for each depth bin, and each depth level is offset by one cell. Therefore, the algorithm is most accurate and bias is at a minimum in the region where there are substantial changes (i.e. offset by one cell) in temperature with depth, in our example, between the depths of 50–200 m (Fig. 2b). Thus when the fish depth-distribution maximum overlaps with the region of minimum bias (i.e. DP3), the overall bias will be less than when the fish depth-distribution maximum does not coincide with the region of minimum bias (i.e. as in DP2).

		Temperature variation ( $\sigma$ )			
		0.25	0.5	1.0	2.0
(a)					
Normal	DP1	2.8 (1.80)	16.3 (6.82)	32.1 (8.11)	46.8 (7.94)
	DP2	4.4 (2.9)	16.2 (6.51)	32.9 (7.78)	47.6 (7.70)
	DP3	1.4 (1.07)	14.7 (5.85)	28.5 (7.35)	41.3 (7.16)
Triangle	DP1	2.7 (1.85)	14.3 (5.56)	26.7 (7.26)	40.5 (6.83)
	DP2	4.4 (2.9)	14.0 (5.22)	26.8 (6.77)	40.3 (6.58)
	DP3	1.4 (1.11)	14.3 (5.30)	27.3 (7.73)	39.8 (7.27)
Uniform	DP1	3.1 (2.73)	62.1 (2.73)	111.5 (9.21)	134.9 (8.58)
	DP2	4.5 (3.39)	71.6 (9.38)	125.7 (10.06)	148.0 (9.05)
	DP3	1.5 (1.5)	46.7 (8.51)	76.2 (8.70)	94.5 (7.75)
(b)					
Normal	DP1	0.54 (0.36)	2.0 (0.96)	3.8 (1.26)	3.9 (0.99)
	DP2	0.94 (0.63)	1.9 (0.95)	3.9 (1.30)	4.0 (0.99)
	DP3	0.26 (0.26)	1.8 (0.95)	3.4 (1.16)	3.4 (0.95)
Triangle	DP1	0.54 (0.38)	1.8 (0.89)	3.3 (1.20)	3.6 (0.93)
	DP2	0.95 (0.63)	1.6 (0.72)	3.1 (1.03)	3.8 (0.94)
	DP3	0.26 (0.27)	1.8 (0.85)	3.3 (1.20)	3.4 (0.96)
Uniform	DP1	0.61 (0.59)	6.1 (1.67)	11.1 (1.25)	8.33 (1.05)
	DP2	0.97 (0.72)	7.2 (1.29)	13.6 (1.88)	9.5 (1.78)
	DP3	0.30 (0.35)	3.9 (0.93)	6.7 (1.20)	6.0 (0.96)

**Table 1.** Mean and standard deviation (SD) of sum absolute difference (Sm, A) and maximum absolute difference (Mx, B) between the estimated depth–temperature matrix (DTMX) and the 'real' depth–temperature matrix (DTM) from 1000 simulations for each scenario. The units are number of minutes per 6-h time interval. Possible values range from 0 to 360 min.

**Table 2.** The average DTMX estimated from satellite-transmitted depth and temperature histograms, and depth-temperature profile data of blue marlin.

Depth (m)	Temperature (°C)											
	<12	12.1–14	14.1–16	16.1–18	18.1–20	20.1–22	22.1–24	24.1–26	26.1–28	28.1–30	30.1–32	>32
0:00–5:59 GMT												
0–25									0.0	314.3		
26–50									1.2	3.2		
51–75								1.7	11.6	1.4		
76–100								14.4	2.6	0.1		
101–125							1.1	7.6	0.1			
126–150							0.4	0.1				
151–175						0.2	0.1					
176–200												
201–225												
226–250												
>250												
6:00–11:59 GMT												
0–25										264.4		
26–50								0.0	0.7	52.7		
51–75								0.5	9.3	18.0		
76–100								3.0	3.0	0.2		
101–125							0.6	1.4	0.0			
126–150						0.0	0.9	0.1				
151–175						1.0	1.7					
176–200					0.2	0.9						
201–225					0.8	0.6						
226–250												
>250					0.1							
12:00–17:59 GMT												
0–25									0.5	60.4		
26–50									2.3	170.9		
51–75								0.9	28.2	41.6		
76–100							0.3	6.9	3.8	0.1		
101–125							8.0	8.1	0.2			
126–150						0.1	9.1	0.6				
151–175						3.8	2.7	0.1				
176–200					0.2	3.7	0.1					
201–225				0.1	2.8	1.0						
226–250					1.8							
>250					1.6							
18:00–23:59 GMT												
0–25									0.0	129.8		
26–50									3.5	153.5		
51–75								0.6	16.2	29.9		
76–100								7.5	4.5	0.1		
101–125							1.1	6.2	0.1			
126–150						0.0	3.5	0.2				
151–175						0.5	1.5	0.0				
176–200					0.0	0.4	0.1					
201–225					0.4	0.0						
226–250					0.3							
>250												

Comparing  $S_m$  values for the three initial temperature distribution functions used in estimations, the uniform distribution performed the worst, and the triangle distribution performed slightly better than the normal distribution although the 'true' DTM was generated with a normal distribution function. The values of  $M_x$  (Table 1b) indicated that the bias for any individual cell was small for all scenarios, especially under normal and triangle initial temperature distributions (<4 min per 6-h interval).

In the recovered tag data comparison, we also estimated the DTMX with three initial temperature distribution functions, and calculated the  $S_m$  and  $M_x$  for each of the 152 pairs of estimated DTMX and the true DTM. To show the performance of the algorithm against the observed data,  $S_m$  and  $M_x$  values were summarized with histograms (Fig. 4a,b). Under all three initial temperature distribution functions, 55% of the estimations had both  $S_m$  and  $M_x$  values equal to 0 (no difference at all) and about 90% of the estimations had  $S_m$  values <20 min and  $M_x$  values <4 min per 6-h interval. Similar to the simulation experiment, the differences between triangle and normal functions were very small, and the uniform function performed worst. With triangle and normal

initial functions, 100% of the estimations had  $S_m$  values <50 min and  $M_x$  values <11 min, and with the uniform initial function, about 4% of the estimates had bias higher than those values. The small across-the-board bias contributes to the small temperature variation in the observed data. From the recovered tag data, we calculated the temperature standard deviation ( $s_t$ ) for each depth bin, and then calculated the average and maximum of  $s_t$  for each observed DTM. The average  $s_t$  (Fig. 5a) is <0.3 (°C) for about 50% of DTM and the maximum  $s_t$  (Fig. 5b) is <1.0 (°C) for about 90% of DTM, which explains the good performance of the algorithm for the observed data.

As the triangle initial temperature distribution function does not require any approximation of  $\sigma$  or truncation at the tails and it produced the least bias in computer-simulated data, we will present the matrix results estimated from this function from here on. It is impractical for us to show all 152 pairs of DTMX in this paper, thus we averaged the DTMX and DTM over 38 days for each 6-h time interval (Tables 2 and 3 and Fig. 6; note that sunset corresponds to approximately 0 hours Greenwich Mean Time (GMT) for the eastern Caribbean Sea during the deployment period). We also calculated the ADM between each pair of DTMX

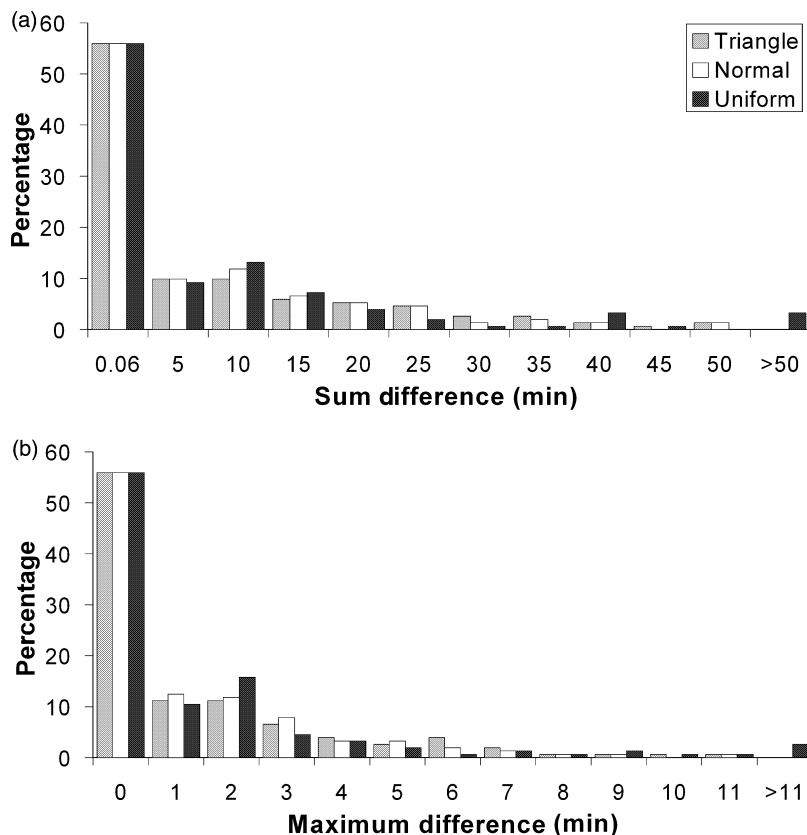


**Figure 4.** Frequency distributions of the sum (a) and maximum (b) absolute differences (minutes per 6 h) between the estimated DTMX and the true DTM from a recovered PAT tag under three initial temperature distribution functions (normal white bar, triangle gray bar, uniform black bar).

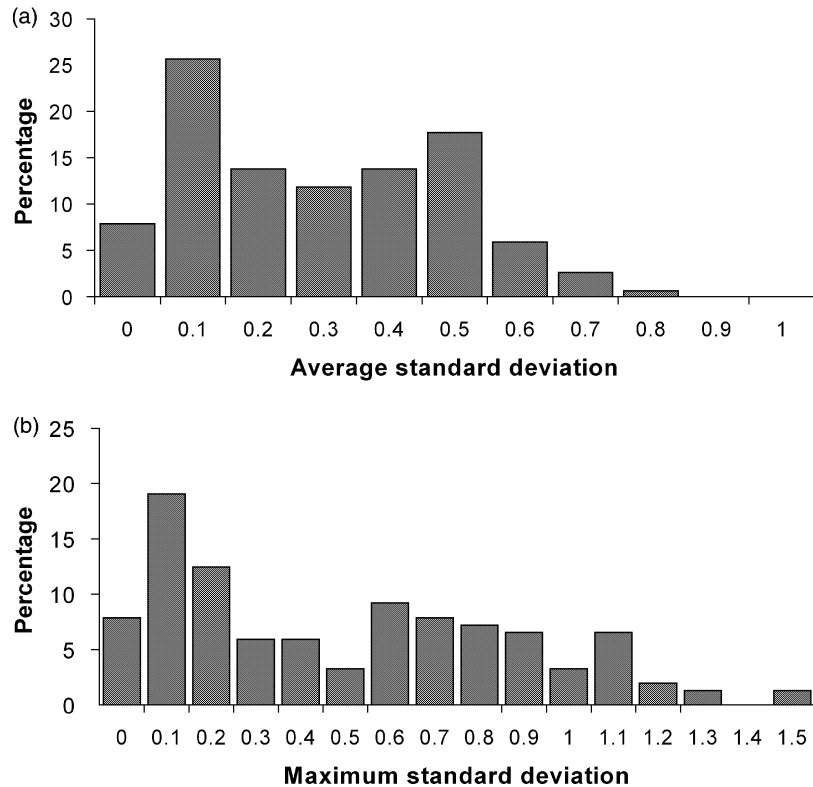


**Figure 5.** Frequency distributions of the average (a) and maximum (b) temperature standard deviation ( $^{\circ}\text{C}$ ) calculated from the recovered PAT tag for each depth bin.

and DTM for each time block and each day, then calculated average matrix and maximum matrix of ADM over 38 days. Comparison of results indicates very small differences between the average DTMX and DTM (Tables 2 and 3 and Fig. 6). Specifically, the average absolute differences over the 38 days were  $\leq 0.6$ , 0.6, 1.3, 1.4 min per 6 h for all cells for the four time periods presented in Table 4, and with a sum of 3.5, 3.0, 13.4 and 7.4 min per 6-h difference over all cells for each time period, respectively. The maximum absolute difference over the 38 days (Table 5) indicates the maximum estimation bias over the 38 days for each cell, and the maximum values for each time period were 8.6, 4.7, 10.2, and 6.6 min per 6 h, respectively. Analysis of the patterns of average and maximum absolute difference indicated that the maximum bias occurred between 50 and 100 m depth, which corresponded to the thermocline of the water column (Fig. 1a) where the maximum temperature variation occurred.

Both DTM and DTMX indicate the same general diel pattern of vertical habitat use by the tagged fish. During complete darkness (i.e. 00:00–05:59 GMT), the blue marlin spent most of its time in the uppermost layer of the water column (0–25 m) where temperatures ranged from 28 to 30 $^{\circ}\text{C}$ , and the average time it spent in waters >150 m was <1 min (0.3 min) during

this time window. During the next time period (i.e. 06:00–11:59 GMT), which included both night and early morning hours, the fish began expanding its vertical and thermal range (5.3 min). By the third, late morning–afternoon time period (i.e. 12:00–17:59 GMT), the fish spent about 18 min at depths >150 m where water temperatures ranged from 18 to 24 $^{\circ}\text{C}$ . Finally, by the late afternoon–evening time period (i.e. 18:00–23:59 GMT), time spent in  $\geq 150$ -m, 18–24 $^{\circ}\text{C}$  water was reduced to about 3 min.

Data from TDRs allowed us to construct a similar DTM for a fishing gear (Table 6; Fig. 7). Element-to-element multiplication of the two matrices provides potential overlap time (as overlap minutes per 6-h interval) between fish and gear (Table 7, Fig. 8). It is assumed here that the gear was fished during each of the four, 6-h time periods. Again, the scenario is examined purely for illustrative purposes – in reality, the experimental gear and the fish tag deployment were separate, independent efforts. Both total (theoretical) time of fish-gear overlap (i.e. the sum of all cells) as well as where in the water column and at what temperatures the overlap occurs can be gleaned in this manner. In our example, there are 14 min of fish-gear overlap assuming fishing was conducted during the first time period (0:00–05:59 GMT). Minutes of overlap for each

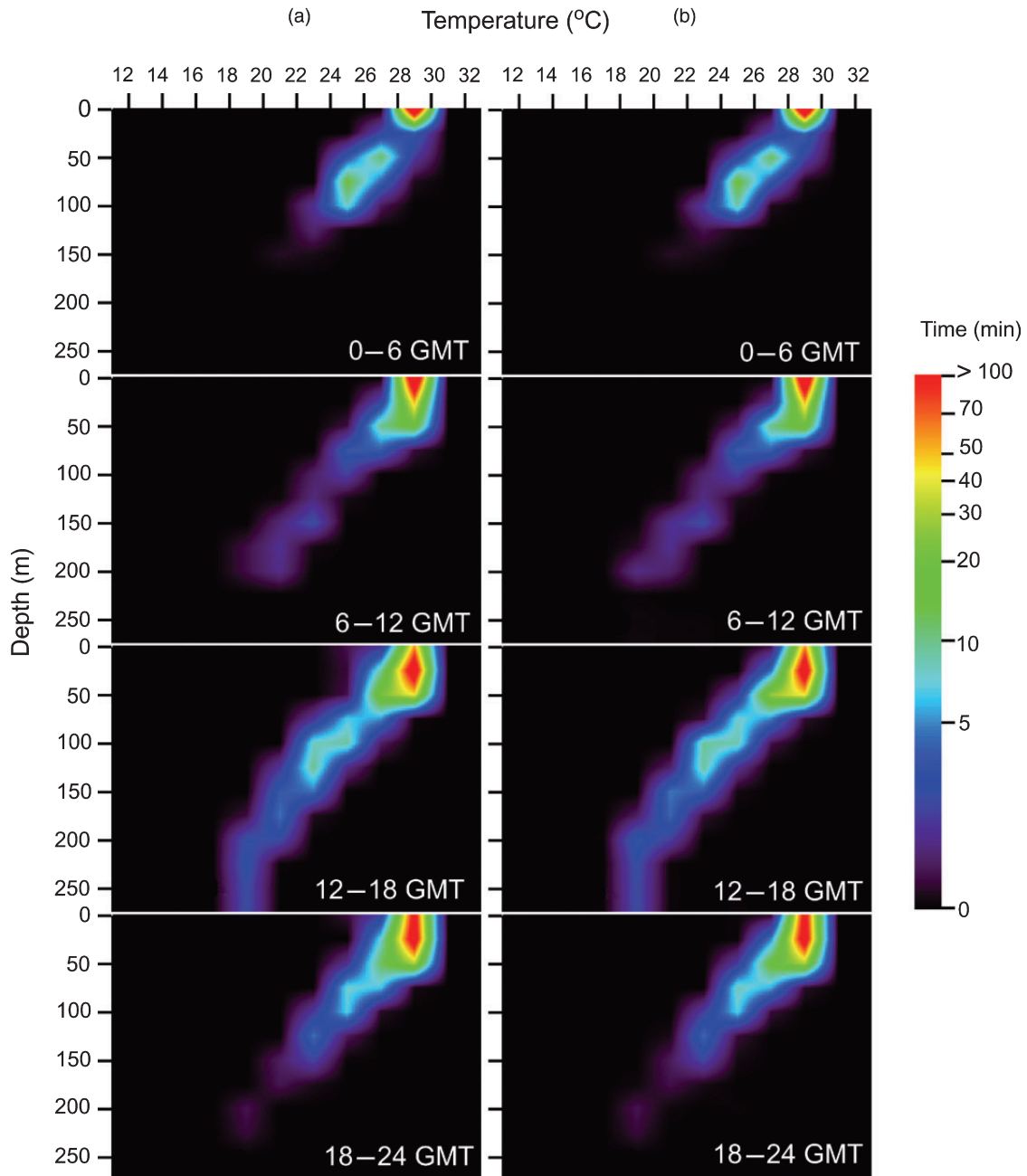
**Table 3.** The average DTM calculated from minute-by-minute data obtained via physical recovery of the PAT tag.

Depth (m)	Temperature (°C)											
	<12	12.1–14	14.1–16	16.1–18	18.1–20	20.1–22	22.1–24	24.1–26	26.1–28	28.1–30	30.1–32	>32
0:00–5:59 GMT												
0–25									0.1	314.2		
26–50									1.3	3.2		
51–75								1.7	11.4	1.5		
76–100								14.4	2.6	0.1		
101–125							1.2	7.5	0.1			
126–150							0.4	0.1				
151–175						0.2	0.1					
176–200												
201–225												
226–250												
>250												
6:00–11:59 GMT												
0–25											264.4	
26–50									0.8	52.6		
51–75								0.5	9.2	18.1		
76–100								2.9	3.0	0.3		
101–125							0.6	1.3	0.1			
126–150						0.1	0.8	0.1				
151–175						0.9	1.7					
176–200					0.2	0.9						
201–225					0.8	0.6						
226–250												
>250					0.1							
12:00–17:59 GMT												
0–25									0.3	60.6		
26–50									3.4	169.8		
51–75								1.2	27.1	42.4		
76–100							0.3	6.7	3.8	0.2		
101–125							8.4	7.6	0.3			
126–150						0.5	8.3	0.9				
151–175						3.6	2.9	0.1				
176–200					0.5	3.3	0.2					
201–225					2.6	1.3						
226–250					1.8							
>250					1.6							
18:00–23:59 GMT												
0–25									0.2	129.7		
26–50									4.0	153.1		
51–75								1.2	15.3	30.3		
76–100								7.2	4.7	0.2		
101–125							1.3	5.8	0.3			
126–150						0.1	3.3	0.3				
151–175						0.4	1.4	0.1				
176–200					0.1	0.3	0.1					
201–225					0.4	0.1						
226–250					0.3							
>250												

subsequent 6-h time interval are 31, 77 and 70 min, respectively. The percent of overlap time ranged from 3.9% to 21.4% with an average of 13.3%

(Table 8), with the greatest amount of overlap occurring during daylight hours and the least during darkness.

**Figure 6.** The average estimated DTMX (a) and the average true DTM (b). The color scale indicates time ranging from 0 to 100 min.



## DISCUSSION

Presented here are (i) a quantitative framework for defining vertical habitat utilization (vertical habitat envelopes) of large marine animals based on data recovered from electronic tags, and (ii) a numerical estimation method for construction of vertical habitat envelopes when only summary data generated by

the WC-PAT tag are available. The vertical habitat envelope framework and the associated estimation method allow for the integration of the thermal and depth preferences of PAT-tagged animals in such a way that vertical habitat use comparisons are simplified to reduced sets of tabular matrices. These matrices are conducive for the study of animal behavior and for calculation (and visualization) of

**Table 4.** The average DTM calculated from minute-by-minute data obtained via physical recovery of the PAT tag.

Depth (m)	Temperature (°C)											
	<12	12.1–14	14.1–16	16.1–18	18.1–20	20.1–22	22.1–24	24.1–26	26.1–28	28.1–30	30.1–32	>32
0:00–5:59 GMT												
0–25									0.1	0.1		
26–50									0.2	0.2		
51–75								0.5	0.6	0.3		
76–100								0.5	0.6	0.0		
101–125							0.1	0.1	0.1			
126–150							0.1	0.1				
151–175						0.0	0.0					
176–200												
201–225												
226–250												
>250												
6:00–11:59 GMT												
0–25											0.1	
26–50									0.3	0.4		
51–75								0.1	0.6	0.5		
76–100								0.1	0.2	0.1		
101–125							0.1	0.1	0.0			
126–150						0.0	0.1	0.1				
151–175						0.1	0.0					
176–200					0.0	0.0						
201–225					0.0	0.0						
226–250												
>250					0.0							
12:00–17:59 GMT												
0–25									0.5	0.5		
26–50									1.1	1.1		
51–75								0.6	1.3	1.2		
76–100							0.2	0.5	0.7	0.2		
101–125								0.5	0.6	0.2		
126–150						0.4	0.8	0.4				
151–175						0.4	0.4	0.0				
176–200					0.3	0.5	0.2					
201–225				0.0	0.3	0.3						
226–250					0.0							
>250					0.0							
18:00–23:59 GMT												
0–25									0.2	0.2		
26–50									0.7	0.6		
51–75								0.6	1.1	0.8		
76–100							0.0	0.7	0.7	0.1		
101–125								0.2	0.4	0.2		
126–150						0.1	0.2	0.1				
151–175						0.1	0.1	0.1				
176–200					0.0	0.1						
201–225					0.0	0.0						
226–250					0.0							
>250												

degrees of overlap – be it among individuals, species or fishing gear. The method, when applied to summary data, produced DTM matrices that were virtu-

ally identical to those produced from the much larger, un-summarized data set. This was encouraging because data summarization is currently a necessity

**Table 5.** The maximum absolute difference between the estimated DTMX and calculated DTM.

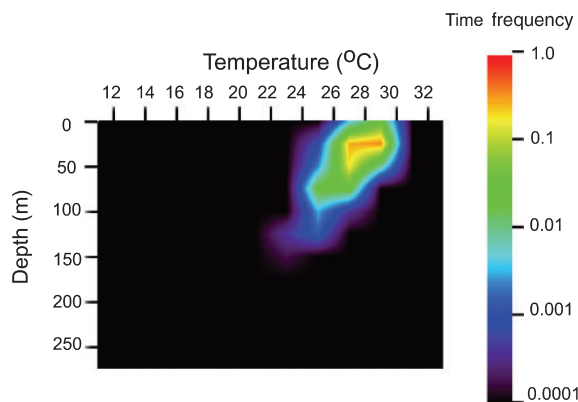
Depth (m)	Temperature (°C)											
	<12	12.1–14	14.1–16	16.1–18	18.1–20	20.1–22	22.1–24	24.1–26	26.1–28	28.1–30	30.1–32	>32
0:00–5:59 GMT												
0–25									1.0	1.0		
26–50									2.0	2.0		
51–75								8.1	6.1	2.0		
76–100								8.1	8.1	0.9		
101–125							1.0	1.9	1.9			
126–150							1.0	1.0				
151–175						0.0	0.0					
176–200												
201–225												
226–250												
>250												
6:00–11:59 GMT												
0–25											1.4	
26–50									4.7	4.7		
51–75								1.0	4.7	4.7		
76–100								1.1	1.4	1.4		
101–125							1.0	2.0	0.9			
126–150						0.9	1.9	1.0				
151–175						1.0	1.3					
176–200					0.0	0.5						
201–225					0.2	0.0						
226–250												
>250	1.3											
12:00–17:59 GMT												
0–25									6.5	6.2		
26–50									8.2	7.6		
51–75								3.8	10.2	8.3		
76–100							3.1	2.5	5.4	1.7		
101–125							2.5	3.5	1.7			
126–150						7.0	9.3	2.5				
151–175						7.0	7.0	0.9				
176–200					2.0	3.6	1.6					
201–225			1.0		2.0	2.0						
226–250					0.9							
>250					1.0							
18:00–23:59 GMT												
0–25									1.0	2.0		
26–50									4.3	4.3		
51–75								6.6	5.8	5.3		
76–100								6.6	6.6	2.0		
101–125							2.8	3.8	2.6			
126–150						1.0	2.8	1.8				
151–175						1.0	1.6	1.0				
176–200					1.5	1.7	1.0					
201–225					1.5	0.9						
226–250					0.0							
>250												

for relatively long-term deployments (i.e. >30 days), and researchers only very rarely physically recover their PAT tags.

Vertical habitat envelopes can be constructed based on data from fishing gear experiments that employ temperature–depth recording devices. Therefore, a

**Table 6.** Hook distribution matrix. The values are percentages of hooks in each cell.

Depth (m)	Temperature (°C)											
	<12	12.1–14	14.1–16	16.1–18	18.1–20	20.1–22	22.1–24	24.1–26	26.1–28	28.1–30	30.1–32	>32
0–25								0.432	2.996			
26–50							0.08	30.327	40.212			
51–75							0.237	18.66	0.954			
76–100							2.683	2.885				
101–125							0.321	0.033				
126–150						0.033	0.137					
151–175						0.008						
176–200												
201–225												
226–250												
>250												

**Figure 7.** The hook depth–temperature distribution. The color scale indicates proportion of time ranging from 0.001 to 1.0.

potentially useful application of this approach is to allow assessment of the possible effects of changing fishing strategies (e.g. fishing deeper or at a different time of day), both on the animals targeted by a given longline fishery and those unintentionally killed as bycatch. While PAT-tag technology is being increasingly applied to more individuals of more species, it is equally important to gather and analyze data on the dynamics of gear behavior.

The simulation evaluation results indicated that differing patterns of fish depth distribution (i.e. unimodal versus bimodal) as well as the assumed initial temperature distribution functions (i.e. uniform, triangle or normal) are relatively unimportant in the estimation of DTM when the temperature variation ( $\sigma$ ) is small. More important is the level of temperature variation within each depth bin which, when high, can lead to unwieldy increases in the number of

cells requiring estimation. Therefore, estimation bias is dependent on the magnitude of temperature variation relative to the temperature and depth bin sizes. Bias is minimized when most of the temperature variation is captured within two bins per depth bin. This was the case in our evaluation of the recovered tag data set wherein 85 of 152 (55%) estimates had exact solutions. Ideally, WC-PAT depth and temperature bins are set before tag deployment with some prior knowledge of the range of depths and temperatures that the study animal utilizes. However, more often than not, the animals 'surprise' us with unexpected behaviors and habitat ranges.

Another limitation of our approach is that the algorithm requires all three types of summary data (i.e., the  $D$ ,  $T$ , and  $DTP$ ) for each time period to estimate the DTM. In many situations only one or two of these summary data types are received for a given time block, thus restricting the number of possible DTMs that can be estimated. In our example, for the 38 days of deployment (at 6-h time interval resolution), the probability of receiving all three summary data types for a given 6-h time period is 83%. Similarly, the transmitted summary data usually have gaps and/or obviously erroneous data values because of interruption of satellite coverage. Before applying our methodology, therefore, appropriate data quality control/assurance steps must be taken. Also, equal bin sizes (except for the first and last bins) are preferable to reduce estimation errors as well as to prevent misinterpretation of results. In situations where bins are not equal, subjective decisions can be used to 're-bin' depth and temperature data into equal intervals; however, this is best avoided at the planning stage of the tag deployment. During tag configuration, both

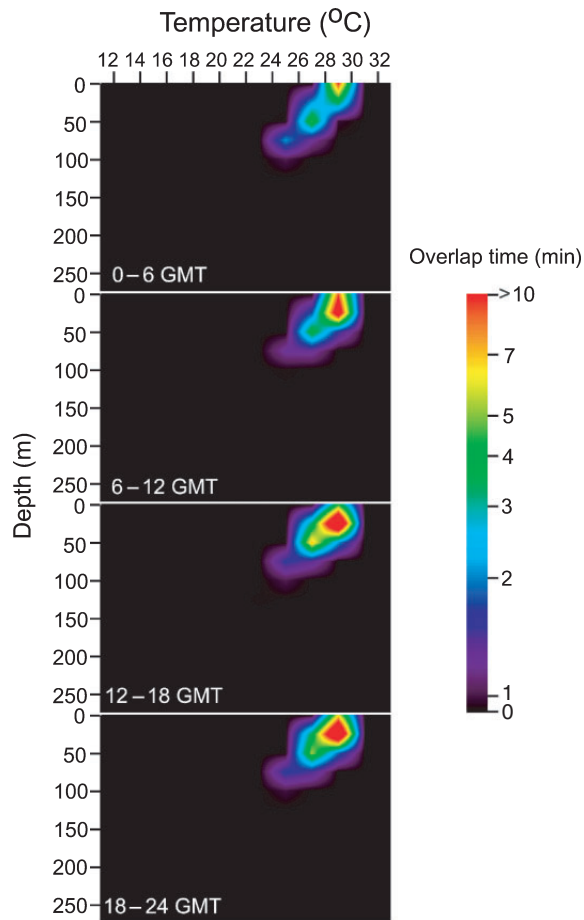
**Table 7.** Potential fish and hook overlap time (minutes) per 6-h time period.

Depth (m)	Temperature (°C)											
	<12	12.1–14	14.1–16	16.1–18	18.1–20	20.1–22	22.1–24	24.1–26	26.1–28	28.1–30	30.1–32	>32
0:00–5:59 GMT												
0–25										9.41		
26–50									0.39	1.27		
51–75									2.13	0.01		
76–100								0.39	0.07			
101–125								0.02				
126–150												
151–175												
176–200												
201–225												
226–250												
>250												
6:00–11:59 GMT												
0–25										7.92		
26–50									0.25	21.14		
51–75									1.72	0.17		
76–100								0.08	0.09			
101–125												
126–150												
151–175												
176–200												
201–225												
226–250												
>250												
12:00–17:59 GMT												
0–25										1.82		
26–50									1.05	68.28		
51–75									5.06	0.40		
76–100								0.18	0.11			
101–125								0.02				
126–150												
151–175												
176–200												
201–225												
226–250												
>250												
18:00–23:59 GMT												
0–25										3.89		
26–50									1.21	61.56		
51–75									2.85	0.29		
76–100								0.19	0.14			
101–125								0.02				
126–150												
151–175												
176–200												
201–225												
226–250												
>250												

the depth and temperature bin sizes should be determined based on available data on the species, the study region and the duration of deployment. The

objective is to cover as much of the full range of depth and temperature as possible for each individual while still having reasonable resolution and consistency for

**Figure 8.** The potential overlap between fishing gear and blue marlin for each time window. The color scale indicates time ranging from 0 to 10 min.



comparisons (e.g. between species, regions, seasons). As stated above, the optimal bin size is to cover most of the temperature variation in two bins. This can be achieved by either increasing the temperature bin size (e.g. from 2 to 3°C) or decreasing the depth bin size (e.g. from 25 to 15 m). Either action represents a trade-off, in resolution or depth range. Fortunately, an important feature of the open pelagic ocean is that

temperature variation is small within certain depth ranges.

Considering the potential utility of the vertical habitat envelope approach, it might be beneficial for DTM calculation to occur directly onboard the next generation of PAT tags and for the DTM to be transmitted via the Argos System *in lieu* of *D*, *T*, and *DTP*. This may be feasible because with the DTM, we can easily reconstruct *D*, *T*, and *DTP* (on land), but only at the resolution of the depth and temperature bins defined initially. While transmission of complete (i.e. 12 × 12) DTM matrices would amount to an increase in message size, transmission of only non-zero DTM cells may, in some cases, represent a reduction.

#### Relevance to pelagic longline fishing

Conceptually, the best fishing strategy is to deploy the greatest number of baited hooks into the foraging habitat of the target species when it is foraging. This approach maximizes encounter probabilities of feeding fish with baited hooks and hence, catch rates. Improvements in fishing strategies with pelagic longlines have been the result of fishers experimenting with bait, hooks, time and place fished, and gear configuration (e.g. length of gangions, length of buoy lines) during the prosecution of the fishery. Currently, pelagic longline configurations vary greatly depending on the species targeted and area fished (Yamaguchi, 1989; Uozumi and Nakano, 1994). On the contrary, the best conservation strategy for non-fishery targeted (i.e. bycatch) species would be to deploy gear such that the greatest numbers of hooks do not overlap the time of day and depths most utilized during foraging. This might result in conflicts between fishing strategy and conservation strategy if each pursues its own objective. By comparing the vertical habitat envelopes of targeted and non-fishery targeted species, we can apply an optimization approach to derive a 'best compromise' strategy for both fishery and conservation.

Comparisons of fish and gear distributions will assist us in assessing the catchability of different gear configurations. Total allowable catches for important

**Table 8.** Summary of potential fish and hook overlap per 6-h time period.

Time period (GMT)	Local time	Total time (min)	Overlap time (min)	Hourly overlap (min/h)	Overlap time (%)
00:00–05:59	7:00 pm–0:59 am	360	14	2.33	3.9
06:00–11:59	1:00 am–6:59 am	360	31	5.17	8.6
12:00–17:59	7:00 am–0:59 pm	360	77	12.83	21.4
18:00–23:59	1:00 pm–6:59 pm	360	70	11.67	19.4
	Average	360	48	8.00	13.3

international fisheries are determined through fish stock assessment analyses. The stock assessments typically use time series of population abundances to evaluate stock status. Often the catch history by longline gear is used to construct catch-per-unit-effort (CPUE) indices for pelagic species that are then used as proxies for the abundance trend. The evolution of the longline fisheries resulted in different catchabilities between gear configurations, locations and time periods. These differences require statistical treatment to remove such effects to produce a 'standardized' series of relative abundances for use in the assessment. However, the extent to which the temporal and spatial variability in gear efficiency is removed by the statistical treatment cannot be directly assessed. The actual overlap of the distributions of the fish and the hooks are essential elements required to directly assess catchability differences among gear configurations, which would be considered as important research priorities (Goodyear *et al.*, 2003).

We suggest vertical habitat envelopes constructed with PAT-tagged fish data and gear experiments may provide concrete data to standardize CPUE in stock assessments. Recent stock assessments of Atlantic marlins conducted by ICCAT indicate that the stock biomass is much reduced from the early years of the fishery and that the stocks are considered to be significantly overfished (Anonymous, 2001). However, applications of recently developed habitat standardization methods (e.g. Hinton and Nakano, 1996; Yokawa *et al.*, 2001; Yokawa and Takeuchi, 2003) that attempt to directly account for the overlap between the species and hooks conflict with the results of the statistical CPUE standardizations used in the assessments (Goodyear, 2003). The different outcomes of the two CPUE standardization approaches foster uncertainty in the status of the stocks and complicate difficult management decisions. The habitat standardizations are currently subject to criticism because of simplistic assumptions about the distribution of the gear and the distribution and behavior of the fish (Goodyear *et al.*, 2003). Also, habitat standardizations with inappropriate assumptions about these distributions can produce misleading results (Goodyear, 2003).

In conclusion, the use of PAT data to define habitat envelopes such as those developed in this paper provides a powerful tool for better understanding the interaction between these species and longline fishing gear. We have presented a method to quantitatively define the degree of overlap between blue marlin habitat and longline fishing gear. This overlap indicates a level of potential interaction (measured as time) that varies by time of day because of the

marlin's diel activity cycle. Accumulation of additional observations will permit analyses of the temperature–depth distributions of this and other large pelagic animals that may lead to models that can predict spatial distributions of multiple species throughout their range. Similar data on the distributions of hooks as a function of gear configuration, locations fished, and other relevant factors may lead to models to predict the vertical distribution of longline hooks by the fishery. Integration of these distributions will likely lead to a better understanding of the interaction of the gear and pelagic animals. Specifically, they might result in better evaluations of temporal trends in the relative abundances of the species using methods based on habitat utilization by the fish and gear (hook) distributions. Additionally, in combination with a greater understanding of the feeding ecology of bycatch species, it may be possible to modify the fishing gear configuration and/or strategy to lower the number of interactions between the gear and bycatch species and thus potentially reduce fishing mortality on non-target stocks. Thus, it may be possible to incorporate the results of vertical habitat envelope analyses into the management process.

## ACKNOWLEDGEMENTS

This work was made possible with Cooperative Research funds of the National Marine Fisheries Service with additional support from The Billfish Foundation and the University of Miami, Center for Sustainable Fisheries, Billfish Research Initiative. We are grateful for the technical assistance provided by Derke Snodgrass, Patrick Rice, Eric Orbesen and Carlos Rivero. Jim Lambert, *F/V Reel Tight* owner, provided financial and logistical support for tag deployment. The captains and crews of the *F/V Reel Tight* and the *F/V Carol Ann* were instrumental in the success of our fieldwork. This paper was greatly improved as a result of the critiques provided by two anonymous reviewers. Clay Porch, Sheryan Epperly and Beth Gardner also provided constructive criticism of an early version of this paper. This paper is Sustainable Fisheries Division contribution No. SFD-2004-028.

## REFERENCES

- Anonymous (2001) Proceedings of the fourth billfish workshop. *Col. Vol. Sci. Pap. ICCAT*. 53:375–400.
- Baskin, J. T. (1986) *Probability: a Noncalculus Introduction*. New Jersey: Rowman and Littlefield, 212 pp.
- Block, B.A., Dewar, H., Blackwell, S. *et al.* (2001) Migratory movements, depth preferences, and thermal biology of Atlantic bluefin tuna. *Science* 293:1310–1314.

- Brill, R.W. and Lutcavage, M.E. (2001) Understanding environmental influences on movements and depth distributions of tunas and billfishes can significantly improve population assessments. *Am. Fish. Soc. Symp.* **25**:179–198.
- Brill, R., Lutcavage, M.E., Metzger, G. et al. (2002) Horizontal and vertical movements of juvenile bluefin tuna (*Thunnus thynnus*), in relation to oceanographic conditions of the western North Atlantic, determined with ultrasonic telemetry. *Fish. Bull.* **100**:155–167.
- Goodyear, C.P. (2003) Tests of the robustness of habitat-standardized abundance indices using simulated blue marlin catch-effort data. *Mar. Freshw. Res.* **54**:369–381.
- Goodyear, C.P., Die, D., Kerstetter, D.W., Olson, D.B., Prince, E.D. and Scott, G.P. (2003) Habitat standardization of CPUE indices: research needs. *Col. Vol. Sci. Pap. ICCAT* **55**:613–623.
- Graves, J.E., Luckhurst, B.E. and Prince, E.D. (2002) An evaluation of pop-up satellite tags to estimate post-release survival of blue marlin (*Makaira nigricans*) from a recreational fishery. *Fish. Bull.* **100**:134–142.
- Hinton, M.G. and Nakano, H. (1996) Standardizing catch and effort statistics using physiological, ecological, or behavioral constraints and environmental data, with an application to blue marlin (*Makaira nigricans*) catch and effort data from the Japanese longline fisheries in the Pacific. *Bull. I-ATTC* **21**:171–200.
- Jonson, I.D., Myers, R.A. and Flemming, J.M. (2003) Meta-analysis of animal movement using state-space models. *Ecology* **84**:3055–3063.
- Kerstetter, D.W., Luckhurst, B.E., Prince, E.D. and Graves, J.E. (2003) Use of pop-up satellite archival tags to demonstrate survival of blue marlin (*Makaira nigricans*) released from pelagic longline gear. *Fish. Bull.* **101**:939–948.
- Musyl, M.K., Brill, R.W., Curran, D.S. et al. (2001) Ability of electronic archival tags to provide estimates of geographical position based on light. In: *Electronic Tagging and Tracking in Marine Fisheries. Reviews: Methods and Technologies in Fish Biology and Fisheries*. J.R. Sibert and J.L. Nielsen (eds) Dordrecht: Kluwer Academic Publishers, pp. 343–368.
- Ortiz, M., Prince, E.D., Serafy, J.E. et al. (2003) A global overview of the major constituent-based billfish tagging programs and their results since 1954. *Mar. Freshw. Res.* **54**:489–507.
- Sibert, J.R. and Nielsen, J.L. (eds) (2001) *Electronic Tagging and Tracking in Marine Fisheries. Reviews: Methods and Technologies in Fish Biology and Fisheries*. Dordrecht: Kluwer Academic Publishers, 468 pp.
- Uozumi, Y. and Nakano, H. (1994) A historical review of Japanese longline fishery and billfish catches in the Atlantic Ocean. *Col. Vol. Sci. Pap. ICCAT* **41**:233–243.
- Yamaguchi, Y. (1989) Tuna long-line fishing II: Fishing gear and methods. *Mar. Behav. Physiol.* **15**:13–35.
- Yokawa, K. and Takeuchi, Y. (2003) Estimation of abundance index of white marlin caught by Japanese longliners in the Atlantic Ocean. *Col. Vol. Sci. Pap. ICCAT* **55**:484–501.
- Yokawa, K., Takeuchi, Y., Okazaki, M. and Uozumi, Y. (2001) Standardizations of CPUE of blue marlin and white marlin caught by Japanese longliners in the Atlantic Ocean. *Col. Vol. Sci. Pap. ICCAT* **53**:345–355.

## APPENDIX

## Appendix 1. Computer code written in IDL for estimation of depth temperature matrices.

```

; NAME:
; MAKE_DTMX. This procedure is written with IDL (Interactive Data
; Language, Research System, Inc. http://www.rsinc.com).
;
; PURPOSE:
; Estimate a depth and temperature matrix DTM=fltarr(nc,nr) from the
; depth histogram D=ftarr(nr), temperature histogram T=fltarr(nc) and
; depth-temperature profile DTP=fltarr(2,nr).
;
; CATEGORY:
; Data simulation.
;
; CALLING SEQUENCE:
; MAKE_DTMX, D, T, DTP, DTMX, TYPE
;
; INPUTS:
; D: array of (nr) elements of the depth histogram.
; T: array of (nc) elements of temperature histogram.
; DTP: array of (2,nr) elements of the minimum and maximum temperature
; for each depth bin.
;
; OPTIONAL INPUT PARAMETERS:
; TYPE: If this parameter is omitted or 0, it will use a normal function
; as initial temperature distribution for each depth bin.
; Set this parameter to 1, will use a triangle function.
; Set this parameter to 2, will use a uniform function.
;
; OUTPUTS:
; DTMX: array of (nc, nr) elements of the depth-temperature matrix
;
; PROCEDURE:
; Uses the RANDOMU, RANDOMN, TRIANGLE_N function.
;
PRO MAKE_DTMX, D, T, DTP, DTMX, TYPE

nr=N_elements(d) ;determine # of rows
nc=N_elements(t) ;determine # of columns
dtmx=fltarr(nc,nr) ;define the DTMX
h=fltarr(12) ;a temporary temp distrib for each depth
Ns=360. ;# of minutes in 6 hrs

if n_elements(type) le 0 then type = 0 ;Default if user miss the option

CASE type OF
  0: BEGIN ;normal distribution
    for j=0,nr-1 do begin
      avg=(dtp(1,j)+dtp(0,j))/2. ;mean of normal distribution
      sigma=(dtp(1,j)-dtp(0,j))/4. ;std dev of normal distribution
      if sigma gt 0 then begin
        rt=randomn(seed,Ns)*sigma+avg
        ;call the random normal distribution function
        val=where(rt ge dtp(0,j) and rt le dtp(1,j))
        ;cut off with min and max temp from DTP

        rt=rt(val)
        num=N_elements(rt) ;determine the # between min and max

```

**Appendix 1.** Continued.

```

h=histogram(rt,min=10.,max=32.,bin=2.0)*1./num
                                ;make histogram to match the temp bin size
dtmx(*,j)=d(j)*h                ;initialize the DTMX
endif else dtmx((avg-10)/2.>0,j)=d(j)
endfor; j
END
1: BEGIN                          ;triangle distribution
for j=0,nr-1 do begin
avg=(dtp(1,j)+dtp(0,j))/2.        ;the center of triangle dist
if (dtp(1,j)-dtp(0,j)) gt 0 then begin
rt=triangle_N(dtp(0,j),avg,dtp(1,j),seed,Ns)
                                ;call the random triangle dist function
h=histogram(rt,min=10.,max=32.,bin=2.)/Ns
                                ;make hist. to match the temp bin size
dtmx(*,j)=d(j)*h                ;initialize the DTMX
endif else dtmx((avg-10)/2.>0,j)=d(j)
endfor
END
2: BEGIN                          ;uniform distribution
for j=0, nr-1 do begin
rt=dtp(0,j)+(dtp(1,j)-dtp(0,j))*RANDOMU(seed,Ns)
                                ;call the random uniform dist function
h=histogram(rt,min=10.,max=32.,bin=2.)/Ns
                                ;make hist. to match the temp bin size
dtmx(*,j)=d(j)*h                ;initialize the DTMX
endfor; j
END
ENDCASE
k=0
REPEAT BEGIN                      ;start the recursive iteration
for j=0, nr-1 do begin           ;do the depth iteration
tsum=total(dtmx(*,j))
if tsum gt 0 then dtmx(*,j)=dtmx(*,j)/tsum*d(j)
endfor; j
for i=0, nc-1 do begin          ;do the temperature iteration
dsum=total(dtmx(i,*))
if dsum gt 0 then dtmx(i,*)=dtmx(i,*)/dsum*t(i)
endfor; i
test2=0
test1=0
dl=fltarr(nr)
t1=fltarr(nc)
for i=0, nr-1 do begin         ;calculating the error of D
dl(i)=total(dtmx(*,i))
test1=test1+abs(d(i)-dl(i))
endfor; i
for i=0,nc-1 do begin         ;calculating the errof of T
t1(i)=total(dtmx(i,*))
test2=test2+abs(t(i)-t1(i))
endfor; i
k=k+1
ENDREP UNTIL (test1 lt 0.00001 and test2 lt 0.00001) or k gt 1000 ; Stop until
the condition.

END                               ;end of procedure MAKE_DTMX

```

## APPENDIX 2

*Algorithm validation*

We first used a simple example to validate the process of the algorithm. Assume we have a known DTM of:

$$\text{DTM} = \begin{bmatrix} 0 & 0.15 & 0.02 \\ 0 & 0.55 & 0.08 \\ 0.05 & 0.05 & 0 \\ 0.05 & 0.05 & 0 \end{bmatrix}$$

From this known DTM, we can sum the rows and columns to obtain  $D$  and  $T$ ; DTP index contains the index of the non-zero cells of DTM (array index is from 0 to 2):

$$D = [0.17, 0.63, 0.1, 0.1]$$

$$T = [0.1, 0.8, 0.1]$$

$$\text{DTP}_{\text{index}} = \begin{bmatrix} (1, 2) \\ (1, 2) \\ (0, 1) \\ (0, 1) \end{bmatrix}$$

Next, we use our algorithm to initialize the DTMX0 with the uniform distribution for the non-zero cells indicated by DTP index for each depth bin:

$$\text{DTMX0} = \begin{bmatrix} 0 & 0.085 & 0.085 \\ 0 & 0.315 & 0.315 \\ 0.05 & 0.05 & 0 \\ 0.05 & 0.05 & 0 \end{bmatrix}$$

Now we use the iteration loop of our algorithm to estimate the DTM with DTMX:

Iteration 1

$$\text{DTMX1} = \begin{bmatrix} 0 & 0.136 & 0.021 \\ 0 & 0.504 & 0.079 \\ 0.05 & 0.08 & 0 \\ 0.05 & 0.08 & 0 \end{bmatrix}$$

Iteration 2

$$\text{DTMX2} = \begin{bmatrix} 0 & 0.144 & 0.021 \\ 0 & 0.535 & 0.079 \\ 0.05 & 0.06 & 0 \\ 0.05 & 0.06 & 0 \end{bmatrix}$$

Iteration 5

$$\text{DTMX5} = \begin{bmatrix} 0 & 0.148 & 0.021 \\ 0 & 0.550 & 0.079 \\ 0.05 & 0.051 & 0 \\ 0.05 & 0.051 & 0 \end{bmatrix}$$

Iteration 6

$$\text{DTMX6} = \begin{bmatrix} 0 & 0.149 & 0.021 \\ 0 & 0.551 & 0.079 \\ 0.05 & 0.050 & 0 \\ 0.05 & 0.050 & 0 \end{bmatrix}$$

Although the computer algorithm stopped after 16 iterations, after six iterations the DTMX values only changed at the fourth decimal place. We can see a small difference by comparing DTM with DTMX6:

$$\text{Dif} = \text{DTMX6} - \text{DTM} = \begin{bmatrix} 0 & -0.001 & 0.001 \\ 0 & 0.001 & -0.001 \\ 0 & 0.0 & 0 \\ 0 & 0.0 & 0 \end{bmatrix}$$

This difference exists because there is no unique solution to the above algebra. DTMX6 is just one of the many solutions to this problem; however, it closely estimated the original DTM.